Electronic Supplementary Material (ESI) for Soft Matter.

Supplementary Information for

Rivalry in *Bacillus subtilis* Colonies: Enemy or Family?

Rajorshi Paul[1], Tanushree Ghosh[1], Tian Tang[1], Aloke Kumar[2*]

[1]Department of Mechanical Engineering, University of Alberta, Edmonton, Canada.

[2]Department of Mechanical Engineering, Indian Institute of Science, Bangalore, India.

***Corresponding author email:** alokekumar@iisc.ac.in

I. Experimental Repeatability

The appearance of a demarcation line and merging between the colonies is dependent mainly on the bacterial strain, the media component (nutrient limitation and agar content), the initial separation distance between the colonies, the initial bacterial biomass and maturity of the colony. If the same bacterial strain is used for the experiment with the same experimental parameters, the colony structure should be similar. The colony structure is the characteristic of bacterial strain (species specific property). The interaction between colonies may differ with different strain, different medium component. The bacterial biomass in the inoculum is the key to the rate of colonial growth and the colony maturation. These two features depend on the primary culture and inoculum size. In our experiments the uncertainty of reproducibly and repeatability to bacterial cell count was about 28% for *B. subtilis*. This deviation in inoculum cell count resulted into the effective colony diameter deviation between 5% and 36% recorded on 1% agar over a period of 36 hours post inoculation. For higher concentration of agar media, the deviation was considerably smaller. For 1.5% agar, the deviation was between 15- 23% and for 2, 3 and 5% agar media these were between 3-22%, 1-5%, and 2-22%, respectively.

II. Estimation of Monod's growth parameters

We prepared three sets of *B. subtilis* cultures in 1.5% LB solution and estimated the population growth of the bacteria cultures over time in terms of optical density OD measured at 600 nm wavelength. The growth curve obtained experimentally was fitted with the theoretical Monod's nutrient depletion model to estimate the specific growth rate g_0, the

half-saturation constant k and the yield γ. Figure S1 shows the comparison between the experimental and fitted theoretical growth curves.

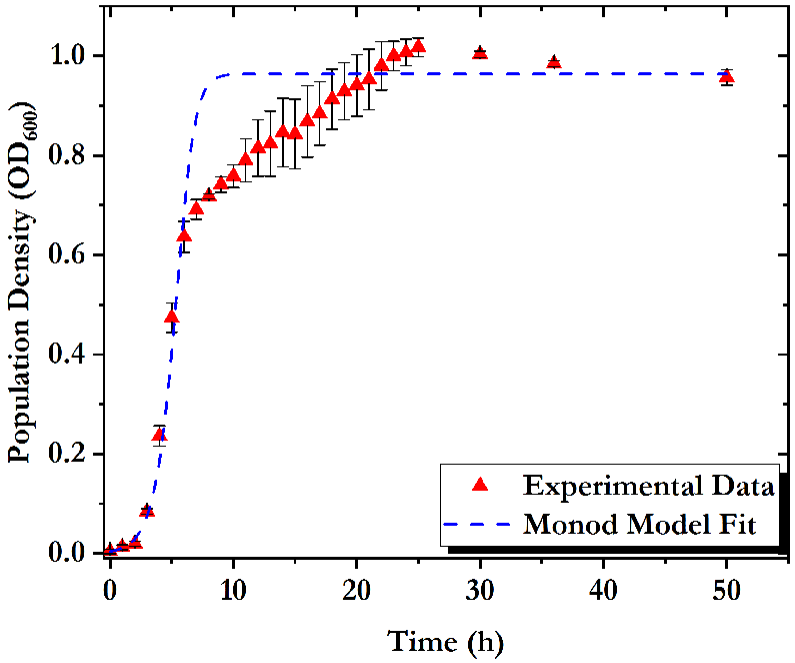

Fig. S1. Experimental growth curve of *B. subtilis* in 1.5% LB solution is fitted with the Monod's model to estimate the growth parameters.

III. Estimation of diffusion coefficient of nutrient

The nutrient source that is used in the experiments consists of a range of different molecules, starting from simple molecules as NaCl to large polymeric protein chains. The molecular weights of the component chemicals vary from 58.5 g/mol to around 2000 g/mol [1]. Based on their molecular weights, each molecule diffuses at different rates. Smaller molecules diffuse faster than large polymers. In a nutrient rich medium such as in the present study, the dynamics of the nutrients will be governed by the slower large molecules. Hence, the effective diffusion coefficient of the nutrient will correspond to that of the massive protein molecules which diffuse very slowly through the growth medium. To estimate the order of magnitude of the effective diffusion coefficient of the nutrient source, we have used Coomassie blue dye (molecular weight 826 g/mol) and measured how the dye spreads over the surface of the growth medium. Figure S2 shows the spreading of the dye over time. As the thickness of the agar in the petri-dish is insignificant compared to the diameter of the petri-dish (~4%), we have considered that the dye diffusion occurs mainly on the agar surface. The dye intensity has been correlated to the dye concentration in MATLAB® which

is finally compared to the two-dimensional diffusion equation for the dye to estimate the order of magnitude of the nutrient diffusion coefficient.

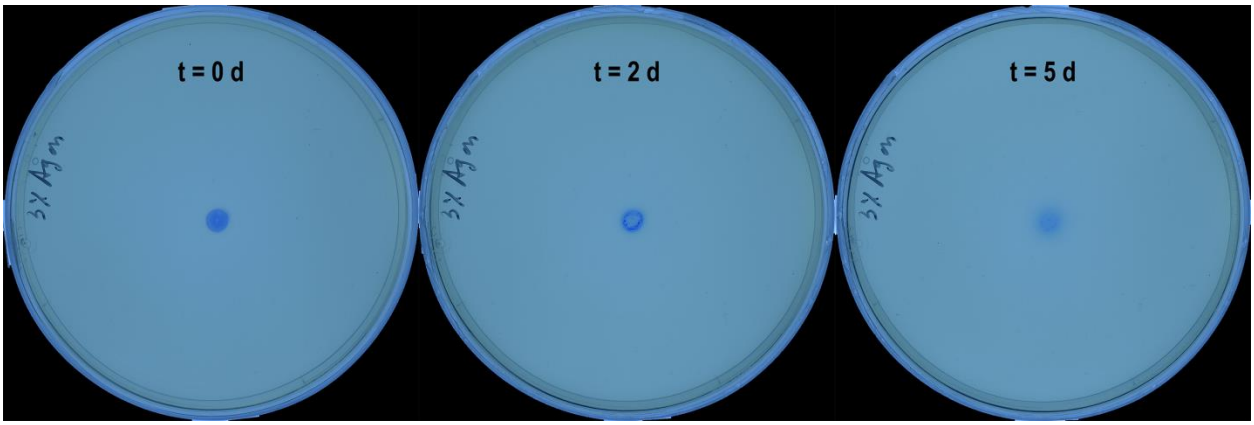

Fig. S2. Diffusion of Coomassie blue dye on 3% agar, 1.5% LB growth medium.

IV. Estimation of diffusion coefficient of colony

To estimate the diffusion coefficient of the bacterial colonies, we compare the numerical solution of the single colony model with the experimental results from single *B. subtilis* colony experiments. We have arbitrarily chosen the initial condition for the bacterial colony to be $X_0 = 10^{-3}$. Based on this initial population, we have defined the population at the colony edge X_e such that the numerical and experimental colony diameters at t = 6 h (post incubation) match. Using thus obtained X_e, we estimate the diffusion coefficient of the colony D_b for the given agar concentration based on the numerical curve which best fits the experimental data. This is shown in Figure 3b of the main article. This is done for different sets of experiments to determine the dependence of the diffusion coefficient with the agar concentration which is shown in Figure S3. The diffusion coefficient at 0.5% agar is nearly one order of magnitude higher than the lowest estimated value which occurs at 2% agar. The diffusion coefficient decreases on increasing the agar concentration from 0.5% till 2%. Beyond 2%, interestingly, for 3% and 5% agar, there is an increase in the value of D_b, which may be caused by excessive production of surfactin by the *B. subtilis* colony. The numerically estimated data are fitted with a polynomial function to determine an explicit correlation between D_b and the reciprocal of the agar concentration (a): $D_b = 5\times10^{-6}a^2 + 1.88a^{-1}$. The quality of the fit measured in terms of the coefficient of determination is $R^2 \approx 98\%$.

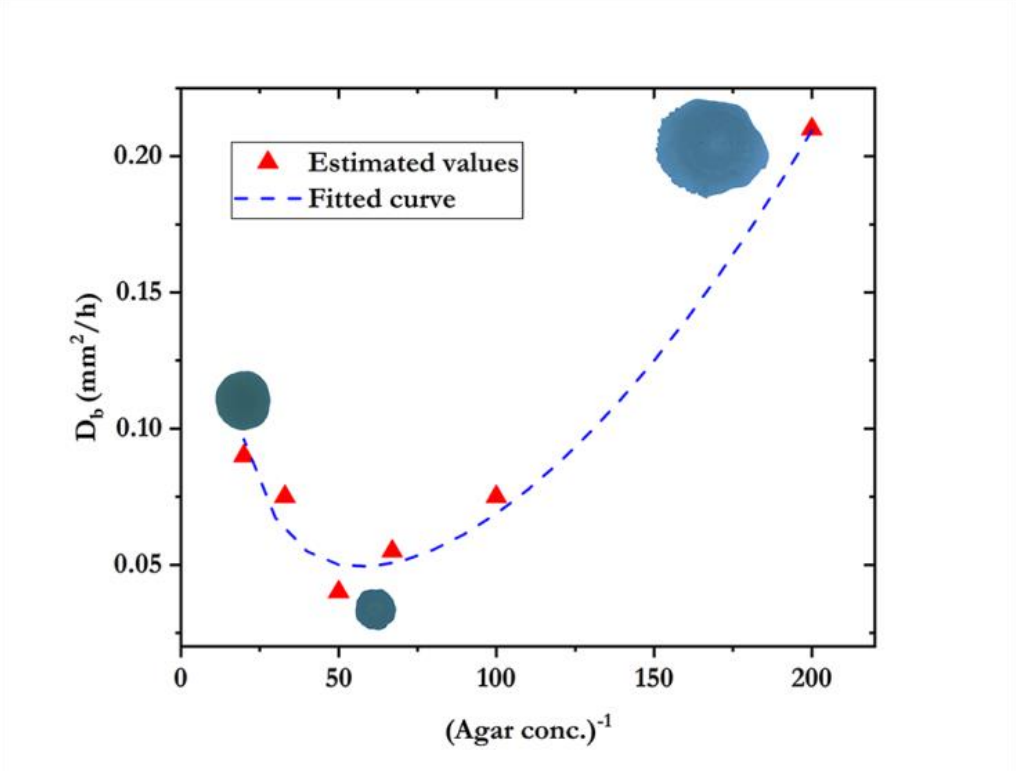

Fig. S3. Estimated diffusion coefficients of the bacterial colony for different agar concentrations in the growth medium. The insets of colonies at 0.5%, 2% and 5% agar correspond to 24 hours post inoculation.

V. Choice of Other Model Parameters

Apart from the Monod growth parameters (g_0, k, γ) and the diffusion coefficients (D_b, D_c), the other parameters required in the proposed model are as follows:

1. X_0: Initial population density in bacterial colony.

   The value of X_0 is essentially the population density of the bacterial culture used for drop casting on the agar plates. Inside a colony it is difficult to measure the population density at different locations. Therefore, in the present study, the population density is a theoretical variable that allows us to determine the colony boundaries for comparison with experiments. As the governing equations are linear, the value of this parameter does not influence the numerical solution of the governing equation. By changing the value of X_0, the solution for the population density is only altered proportionally. Therefore, the value of X_0 is chosen arbitrarily as $X_0 = 10^{-3}$.

2. X_e: Reference population density for demarcating colony boundary

   As the reaction-diffusion models are essentially continuous models, it is necessary to define a reference bacterial population density X_e to demarcate the edge of the colony. This was done by matching the numerical and experimental colony diameters at t = 6 h (post incubation). As the colony diameters are nearly identical on different agar

concentrations at 6 hours (Figure 4.4 in main article), so is the estimate of X_e. The value of X_e was found to lie within 0.1 and 0.3. For the two-colony model, we have chosen $X_e = 0.3$ and this value has been used consistently in all numerical. It is to be noted that the value of X_e depends on the initial population density X_0. On using a different initial population density, the value of X_e will proportionally change so that the ratio X_e/X_0 is constant, in this case $X_e/X_0 = 300$.

3. c_0: Initial nutrient concentration

The initial concentration of the nutrients in the growth medium is 15 g/L of LB. Hence, in the model, $c_0 = 15$ g/L has been used.

4. c^*: Threshold nutrient concentration

The value of the threshold nutrient concentration c^* does not have any notable numerical consequence. In Figure S4, the numerical solutions for the population density X at $t = 30$ h for $D_b = 0.04$ mm^2/h in the single colony model are compared for different values of c^*. The solutions are found to change insignificantly over three orders of magnitude of c^*. Therefore, the value of c^* is chosen as 10% of c_0, $c^* = 1.5$ g/L, as was used by Patra et al. [2].

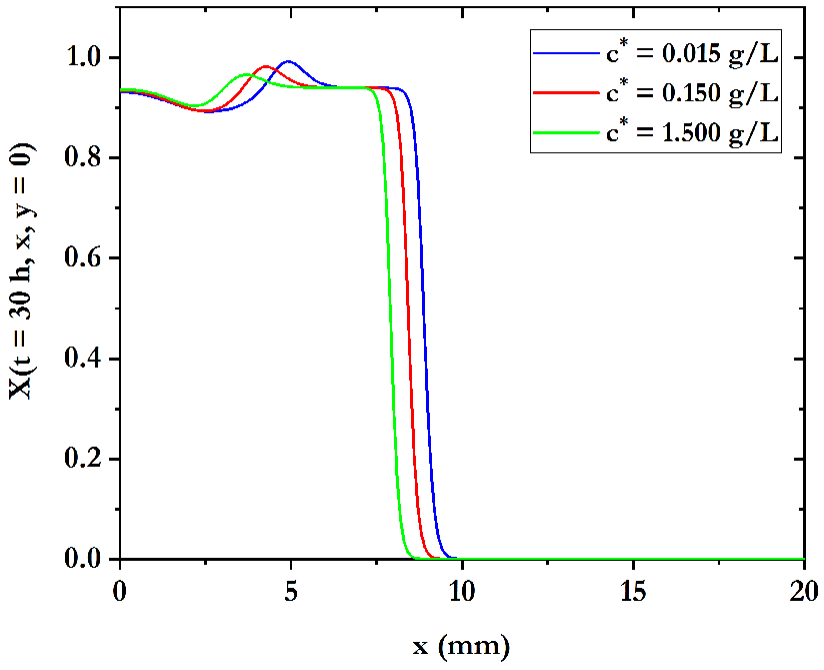

Fig. S4. Influence of c^* on the numerical solution of the single colony model. The solutions for the population density $X(t = 30\text{ h}, x, y = 0)$ are compared for different values of c^*.

5. ρ : Radius of bacterial colony inoculum

The parameter ρ represents the radius of the bacterial colony inoculum resulting from drop casting of 16 hour *B. subtilis* culture. 1 μL of the culture solution was used for the drop casting. The radius of the drop was determined by image processing and based on the estimate, ρ was chosen as $\rho = 2.5$ mm.

6. t^* : Reference time denoting onset of demarcation

The parameter t^* essentially marks the onset of demarcation between sibling colonies. Experimentally, we have found that the demarcation occurs when the agar concentration in the growth medium is high $(\geq 1\%)$. In high agar concentration growth media, experiments show that the line of demarcation starts forming ~24 hours after incubation. On the other hand, the colonies which merged were found to start merging much earlier (at around 20 hours or earlier. Based on these observations, the reference time was chosen as $t^* = 20$ h . To better understand the implication of this parameter, we studied the spreading characteristics of *B. subtilis* colonies at high agar concentrations. Interestingly, approximately around 20 hours post inoculation, there is a change in the spreading rate of the colonies growing on high agar concentration growth media. After 20 hours, the colonies spread at slower rates on the surface of agar. This is shown in Figure S5.

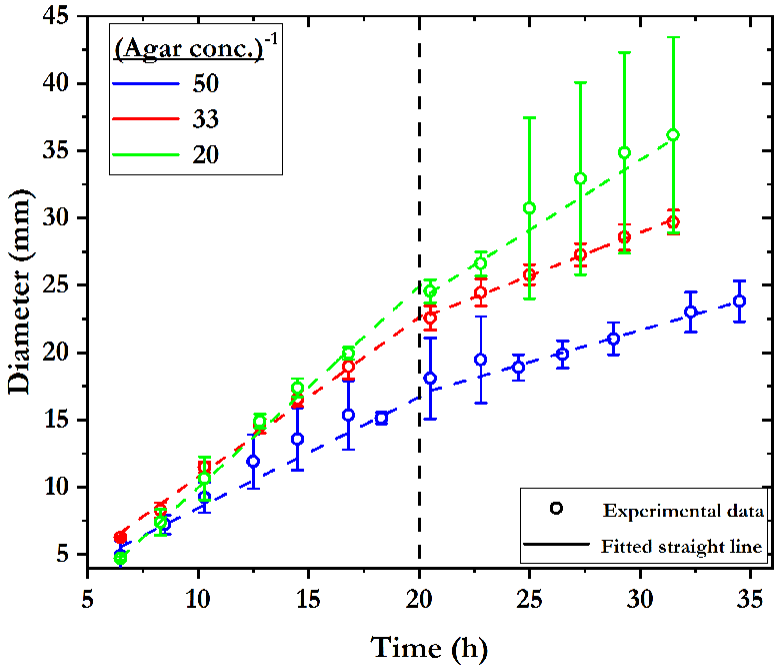

Fig. S5. Growth of *B. subtilis* colonies on high agar concentration media.

7. μ : Mortality coefficient

The parameter μ accounts for the rate at which cell death occurs near the demarcation line between the colonies. Numerically, the coefficient of mortality μ is responsible for generating a stable interface by incorporating the inhibitory interaction between colonies. As there is no direct way of estimating the value of μ experimentally, a parametric analysis of μ has been conducted as shown in Figure S7. In Figure S7 the numerical solutions for the population density X at $t = 30\,\text{h}$ taken along the x axis ($y = 0$) are compared for $\mu = 4\ \text{h}^{-1}\left(\bar{\mu} = 10^{-3}\right)$, $\mu = 40\ \text{h}^{-1}\left(\bar{\mu} = 10^{-2}\right)$ and $\mu = 400\ \text{h}^{-1}\left(\bar{\mu} = 10^{-1}\right)$. For the simulation, $D_b = 0.04\ \text{mm}^2/\text{h}$ and the colony boundary is demarcated by the threshold population density $X_e = 0.3$. For very small values of μ, e.g., $\mu = 4\ \text{h}^{-1}\left(\bar{\mu} = 10^{-3}\right)$, the numerical solution demonstrates that there is no interface generated because the mortality term is negligible. At larger values of μ, $O\left(10^{-2}\right) \le \bar{\mu} \le O\left(10^{-1}\right)$, interfaces can be observed and the results are insensitive to the specific values of μ. Very large values of μ, on the other hand, makes the solution numerically unstable. From the results of the parametric study, μ is chosen to be $\mu = 40\ \text{h}^{-1}$. As the numerical solution remains nearly unaffected by changing the value of the coefficient in the chosen range, it can be reasonably assumed to be a constant.

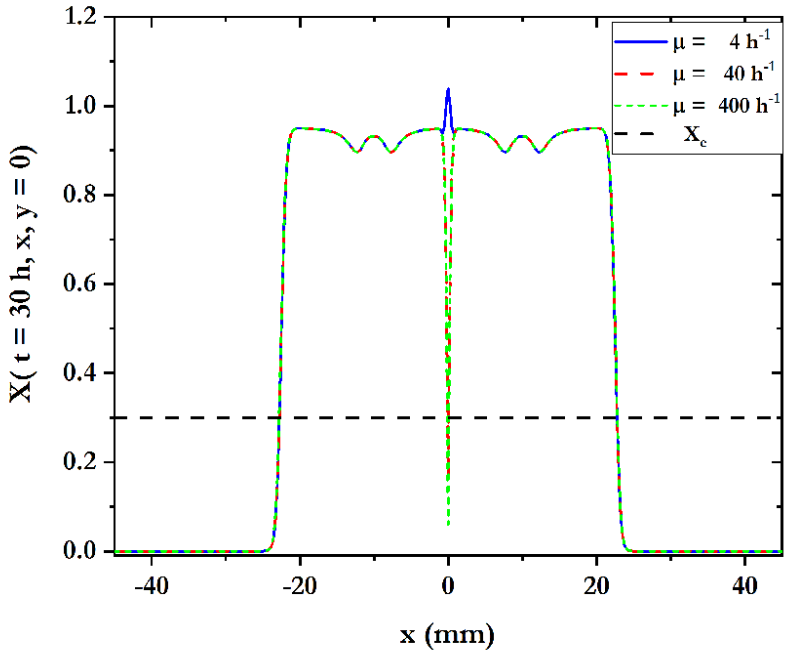

Fig. S6. Influence of μ on the numerical solution. The solutions for the population density $X\left(t = 30\ \text{h}, x, y = 0\right)$ are compared for different values of μ .

VI. Non-dimensionalization

The dimensionless form of the governing equation with initial and boundary conditions are as follows:

$$\begin{aligned}
\frac{\partial \bar{X}_1}{\partial \tau} &= \bar{g}\left(\bar{c}\right)\bar{X}_1 + \bar{\nabla}\cdot\left(\bar{D}\mathcal{H}\left[\bar{c}-\bar{c}^*\right]\bar{\nabla}\bar{X}_1\right) - \bar{\mu}\bar{X}_1\bar{X}_2\mathcal{H}\left[\tau-\tau^*\right]\mathcal{H}\left[\bar{X}^{\Gamma}-\bar{X}\left(\tau,\bar{x}=0,\bar{y}=0\right)\right] \\
\frac{\partial \bar{X}_2}{\partial \tau} &= \bar{g}\left(\bar{c}\right)\bar{X}_2 + \bar{\nabla}\cdot\left(\bar{D}\mathcal{H}\left[\bar{c}-\bar{c}^*\right]\bar{\nabla}\bar{X}_2\right) - \bar{\mu}\bar{X}_1\bar{X}_2\mathcal{H}\left[\tau-\tau^*\right]\mathcal{H}\left[\bar{X}^{\Gamma}-\bar{X}\left(\tau,\bar{x}=0,\bar{y}=0\right)\right] \\
\frac{\partial \bar{c}}{\partial \tau} &= -\bar{\gamma}\bar{g}\left(\bar{c}\right)\bar{X} + \bar{\nabla}\cdot\left(\bar{\nabla}\bar{c}\right)
\end{aligned} \tag{S1}$$

$$\begin{aligned}
\bar{X}_1\left(\tau=0,\left(\bar{x}-\frac{\bar{d}}{2}\right)^2+\bar{y}^2\le\bar{\rho}^2\right) &= \bar{X}_2\left(\tau=0,\left(\bar{x}+\frac{\bar{d}}{2}\right)^2+\bar{y}^2\le\bar{\rho}^2\right)=1 \\
\bar{c}\left(\tau=0,\bar{x},\bar{y}\right) &= 1
\end{aligned} \tag{S2}$$

$$\begin{aligned}
\bar{\nabla}\bar{X}_1\cdot\hat{\mathbf{n}}\big|_{\bar{\Gamma}} &= \bar{\nabla}\bar{X}_2\cdot\hat{\mathbf{n}}\big|_{\bar{\Gamma}} = 0 \\
\bar{c}\big|_{\bar{\Gamma}} &= 1
\end{aligned} \tag{S3}$$

$\frac{1}{g_0}$ and $\sqrt{\frac{D_c}{g_o}}$ non-dimensionalization factors for the time and length scales respectively and the corresponding dimensionless variables are as follows:

$$\tau = g_0 t\,,\ \tau^* = g_0 t^*$$

$$\bar{\rho} = \sqrt{\frac{g_0}{D_c}}\rho\ ,\bar{\nabla} = \sqrt{\frac{D_c}{g_0}}\nabla\,,\ \bar{\rho}_0 = \sqrt{\frac{g_0}{D_c}}\rho_0\,,\ \bar{R} = \sqrt{\frac{g_0}{D_c}}R\,,\ \bar{d} = \sqrt{\frac{g_0}{D_c}}d$$

The dependent variables and parameters related to the population density and the nutrient concentrations are non-dimensionalized in terms of the initial condition as follows:

$$\bar{X}_1 = \frac{X_1}{X_0}\,,\bar{X}_2 = \frac{X_2}{X_0}\,,\ \bar{c} = \frac{c}{c_0}\,,\ \bar{c}^* = \frac{c^*}{c_0}\ \ \bar{k} = \frac{k}{c_0}\,,\ \bar{\gamma} = \gamma\frac{X_0}{c_0}\,,\ \bar{\mu} = \mu\frac{X_0}{g_0}$$

The normalized diffusion coefficient $\bar{D}$ is defined as $\bar{D} = \frac{D_b}{D_c}$.

VII. Interaction of B. subtilis with PDMS and PP structures

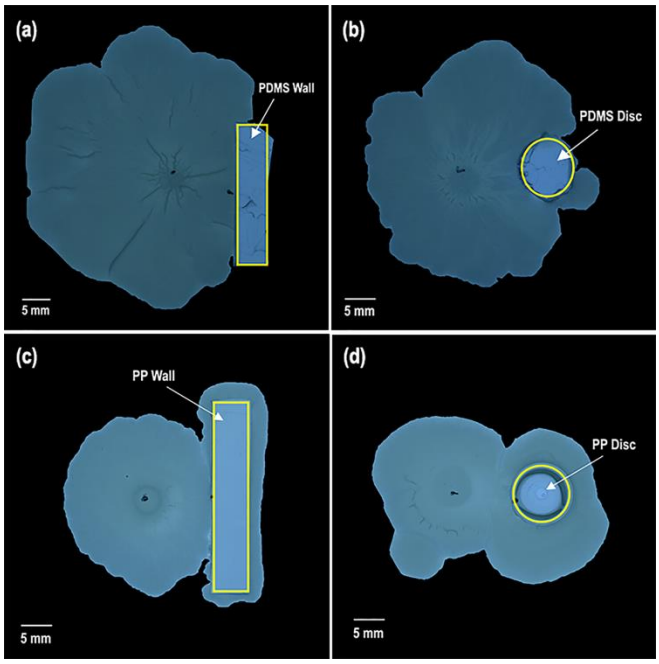

Fig. S7. *B. subtilis* colonies grow and reach the surfaces of the solid PDMS (**a** and **b**) and PP (**c** and **d**) structures. The colony grows completely around the edges of the PP structures. The images **(a)** and **(b)** were taken 48 hours after inoculation. Image **(c)** and **(d)** were taken respectively at 72 and 28 hours after inoculation.

VIII. Inter-colony Interactions

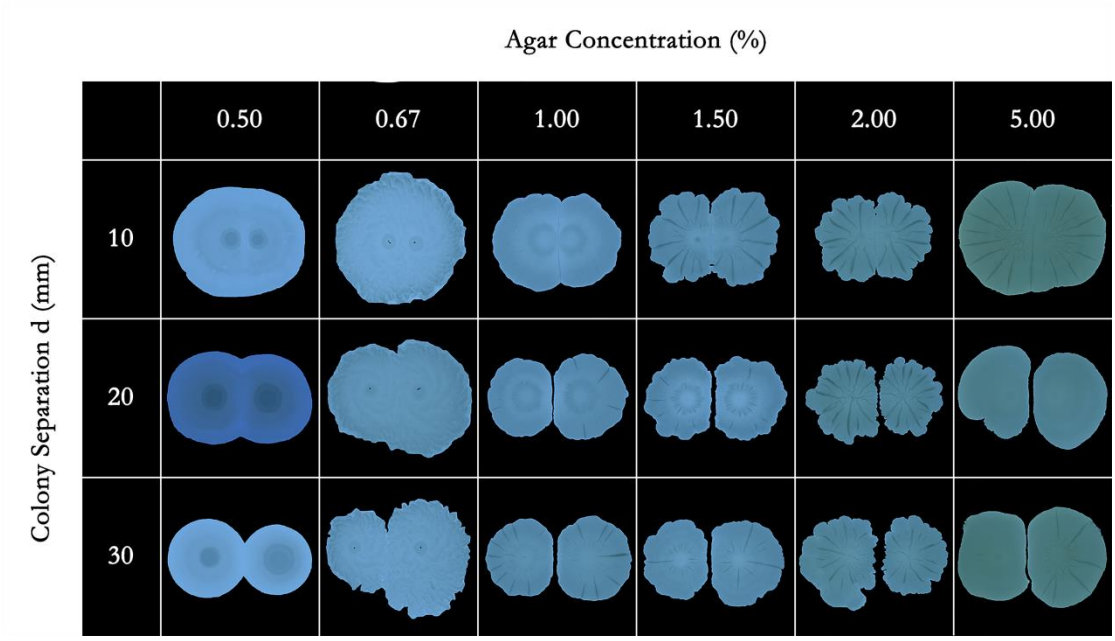

Fig. S8. Images showing the nature of interaction between two sibling *Bacillus subtilis* colonies for different conditions of colony separation and agar concentration.

Supplementary Videos

Supplementary Video 1: Video shows merging of two growing sibling *B. subtilis* colonies. The experiment is performed on 0.5% agar and the initial separation between the colonies is 20 mm. Colonies start merging at around 18 hours post inoculation.

Supplementary Video 2: Video shows merging of two growing sibling *B. subtilis* colonies on 0.5% agar with the initial separation between the colonies 30 mm. In this case colonies start merging at around 20 hours post inoculation.

Supplementary Video 3: Video shows DL formation between two growing sibling *B. subtilis* colonies. The experiment is performed on 2% agar and the initial separation between the colonies is 20 mm. Colonies start forming a DL after 24 hours post inoculation.

Supplementary Video 4: Video shows the progression of *B. subtilis* colonies on agar plates as observed under an inverted optical microscope. The video shows three different colonies. The first colony was grown on 0.5% agar and the colony progression was recorded continuously for 5 minutes. The second colony was grown on 2% agar and the video segment shows how the colony matures over a period of 6 hours from the point of inoculation. The third colony was also grown on 2% agar. The video segment shows the progress of a mature *B. subtilis* colony over 30 minutes.

References:

1. Production, BD Biopharmaceutical. "Bionutrient technical manual." (2004).
2. P. Patra, C. N. Vassallo, D. Wall and O. A. Igoshin, *Biophys J*, 2017, **113**, 2477-2486.